Published in final edited form as:
Brain Res. 2010 March 10; 1319C: 131–141. doi:10.1016/j.brainres.2009.12.089.

Microglial response to murine leukemia virus-induced encephalopathy is a good indicator of neuronal perturbations

Qing-Shan Xue[1], **Cui Yang**[1], **Paul M. Hoffman**[2,3], and **Wolfgang J. Streit**[1]

[1]Department of Neuroscience, University of Florida College of Medicine, McKnight Brain Institute, Gainesville, FL

[2]Department of Neurology, University of Florida College of Medicine, McKnight Brain Institute, Gainesville, FL

[3]Department of North Florida/South Georgia Veterans Health System

Abstract

The neuronal pathology caused by neonatal infection of rats with the PVC-211 murine leukemia virus (PVC-211 MuLV) and its underlying mechanisms are not well defined even though a loss of neurons and spongiform neurodegeneration has been reported to accompany the disease. Here we sought to identify sites of neurodegeneration using microglial reactivity as an indirect marker and to characterize microglial activation during disease progression. Using a panel of microglial antibodies including Iba1, OX-42, ED1, and anti-ferritin, we have studied the response of microglial cells to neonatal CNS infection with PVC-211 at post-infection survival times 7, 14, 21, and 28 days. We found that microglial activation occurred primarily in the spinal cord and brainstem where it gradually increased in intensity over the time course of this study. Other brain areas were relatively unremarkable in their microglial reaction to viral infection within this time frame. However, presence of activated microglial cells was not correlated directly with presence of viral glycoprotein (gp70), which was expressed in endothelial cells throughout the CNS. Although double labeling of microglia with Iba1 and ED1 revealed numerous actively phagocytic microglia during disease progression, not all activated microglia were ED1-positive. In addition to the intense microglial activation, we found increased ferritin expression sporadically throughout the virus-infected brain. The ferritin-positive cells were mostly microglia that exhibited dystrophic changes and likely represented a degenerating subpopulation of microglial cells. Thus, activated microglia can co-exist with degenerating microglia in the same brain region. We attempted to localize degenerating neurons or neurites using Fluoro-Jade, anti-tau, and anti-alpha synuclein staining, but none of these procedures yielded results to indicate obvious neuronal pathology. We conclude that the visualization of microglial activation is a more sensitive measure of neuronal perturbations than direct detection of neuronal pathology which may be subtle and not produce overt degenerative changes.

Keywords

rat; ED1; ferritin; murine leukemia virus; microgliosis

Author for correspondence: Wolfgang J. Streit, Ph.D., Department of Neuroscience, PO Box 100244, University of Florida College of Medicine, Gainesville, FL 32610-0244, Tel.: 352-392-3910, Fax: 352-392-8347, streit@mbi.ufl.edu.

1. Introduction

PVC-211 MuLV is a neuropathogenic, paralysis–inducing virus that produces a neurodegenerative syndrome characterized by tremor, loss of splay reflex, ataxia, and hindlimb weakness/paralysis after intracerebral inoculation into neonatal rats or mice (Hoffman et al., 1992; Kai and Furuta, 1984; Wilt et al., 2000). However, the neuropathology of this infection paradigm is not well defined or even controversial to date. Earlier studies characterized the neuropathology as being noninflammatory with perivascular astrogliosis and marked by development of spongiform vacuolar neurodegeneration where neuronal cell bodies were largely spared and neuronal drop-out was rare (Hoffman et al., 1992; Kai and Furuta, 1984). More recently, neuronal loss was reported to occur in the cerebellum and brainstem during end stage disease (Li et al., 2009). In addition, activation of microglia has been reported (Wilt et al., 2000) indicating that while not a blatantly inflammatory condition, an endogenous neuroinflammatory component does exist. In light of these disparate findings, we sought to further characterize the neuropathology of PVC-211 infection by performing a comprehensive analysis of microglial reactivity with a number of cell markers.

In previous studies (Li et al., 2009; Wilt et al., 2000), the microglial reaction to neonatal PVC-211 infection, was assessed using immunostaining with ED1 antibody, which is a macrophage marker that recognizes an intracytoplasmic, lysosomal antigen whose expression increases during phagocytic activity in monocytes and other tissue macrophages, including in microglia (Bauer et al., 1994; Dijkstra et al., 1985; Graeber et al., 1998). Thus, the endogenous neuroinflammatory response in PVC-211-infected rats has not been characterized with markers directed against microglial surface antigens to delineate non-activated (resting), as well as activated but non-phagocytic microglia which are ED1-negative (Graeber et al., 1998). Visualization of all microglial activation states is important for better characterizing the extent and nature of neurodegenerative changes since these cells are known to be sentinels of even subtle pathological alterations in neurons (Kreutzberg, 1996). Hence we employed two universal microglial antibodies, Iba1 and OX-42, to display all the microglial cells, and to co-display ED1 expression in the microglia by double labeling techniques. In addition, we used immunohistochemistry for the iron storage protein, ferritin, to further characterize the microglial response. Ferritin is an interesting marker for microglia because the significance of its expression is not well understood. While its expression has been shown to be upregulated on ostensibly activated microglia in animal studies of ischemia and epilepsy (Gorter et al., 2005; Ishimaru et al., 1996), other studies in human tissues show a preferential expression of ferritin on dystrophic rather than on activated microglia (Lopes et al., 2008; Simmons et al., 2007). Dystrophic microglia are thought to be senescent and thus degenerating cells, and their appearance in human brain can be closely correlated with neurodegenerative changes (Streit et al., 2004; Streit et al., 2009). Thus, we were interested in finding out whether virally induced neurodegeneration also involves microglial degeneration. In particular, since ferritin-positive microglia are exceedingly rare in the uninjured rat brain, and since PVC-211 MuLV is known to target endothelial cells (Hoffman et al., 1992), we thought it possible that virus-mediated damage to microvessels could produce hemorrhages and therefore higher levels of iron in the CNS that would trigger an upregulation of ferritin.

2. Results

Animals infected with PVC-211 MuLV began to show neurological symptoms to a variable degree at 2-3 weeks post-infection. Symptoms included spastic paresis, ataxia and hind limb weakness that progressed to paralysis, and these occurred in most animals. Histopathological analysis of microglia was performed in coronal sections of the spinal cord and brain from both infected and control animals.

2.1. Microglial development in PVC-211 virus infected brain

Using OX-42 antibody in the spinal cord lumbar enlargement from controls, microglia were observed going through the normal developmental phases of differentiation into fully ramified cells accompanied by a progressive increase in cell density during the first 28 days of postnatal life, as described in detail by others (Kaur et al., 1993) (Figs. 1A, B). At 28 days, microglial distribution and density was essentially as in adults. In PVC-211-infected animals, activated microglia first became apparent as hypertrophic cells at 14 days post-injection (dpi), but these were isolated incidences and for the most part microglial distribution at early time points closely resembled that seen in controls (Figs. 1C, D). Activation of microglia became more obvious at 21 and 28 dpi when hypertrophic cells were found consistently throughout the spinal gray matter of all animals (Figs. 1E, F). Activated microglia were seen to occur diffusely distributed as well as aggregated in clusters (Fig. 2). High magnification clearly revealed increased staining intensity of activated cells and greater cell density in infected versus control animals (Figs. 2A, B). The increased density was due primarily to hypertrophy of individual cells rather than to increased cell numbers (hyperplasia), and there was no evidence of cell division, such as metaphase or telophase nuclei in sections counterstained with cresyl violet despite the fact that cresyl violet staining tended to be stronger in infected brains. Activated microglia were not ensheathing the perikarya of motor neurons, as shown by double-labeling neurons and microglia with NeuN and Iba1 antibodies (Figs. 2C, D). Numbers of NeuN-positive spinal cord neurons were qualitatively comparable in infected and control animals. Clusters of microglia were observed that may have indicated phagocytosis of an occasional dead neuron (Fig. 2D). We attempted to localize degenerating neurons or neurites using Fluoro-Jade, anti-tau, and anti-alpha synuclein staining, but none of these procedures yielded results to indicate obvious neuronal pathology (not shown).

2.2. Brain-area specificity of microglial activation in virus infected brain

Besides the spinal cord which was marked most prominently by microglial activation, diffuse microglial activation as well as occasional clusters also occurred in most of the central portions of the brainstem, and to a lesser extent in cerebellum, midbrain, and cortical/subcortical regions (Fig. 3). Clusters of activated microglia were rare in the cerebellum (Fig. 3D), the cerebral cortex (Fig. 3E), and the hippocampus (Fig. 3F) and seen there in only two out of all the virus infected animals.

To determine the relationship between brain regional specificity of microglial activation and PVC-211 virus distribution, we performed double-labeling for microglia and the viral glycoprotein, gp70. We found that gp70 was expressed widely in endothelial cells throughout the CNS microvasculature but without any predilection for those regions showing the most microglial activation (i.e. spinal cord and brainstem), and that both activated and non-activated microglia were present in the vicinity of gp70-positive microvessels (Fig. 4). Thus, microglial activation was not correlated directly with presence of virus in endothelial cells.

2.3. Not all activated microglia are ED1-positive

To characterize activated microglia in terms of their phagocytotic activity, we employed double-labeling with antibodies Iba1 and ED1. We limited our analysis to late time points (21 and 28 dpi) because during early postnatal development this antigen is expressed widely by so-called ameboid microglia, which are immature microglial precursor cells that exhibit macrophage characteristics. Normally, ameboid microglia completely disappear by postnatal day 21 (Milligan et al., 1991a) due to their differentiation into fully ramified microglia and concomitantly they lose ED1 immunoreactivity. Thus, our control animals were largely devoid of ED1 staining at 21 and 28 dpi (Figs. 5A, C, E). In contrast, ED1 staining was prominent in virus-infected rats and visible as punctate intracellular staining (Figs. 5B, D, F), which upon co-labeling with a universal microglial marker, Iba1, resulted in being co-localized with many

but not all activated microglia (Figs. 5D, F). We interpret these findings to show that some of the activated microglia were engaged in phagocytosis, presumably removing debris resulting from neuronal degeneration.

2.4. Ferritin expression is increased in virus infected brain

To further characterize the microglial response to PVC-211 infection, we employed anti-ferritin immunohistochemistry. Ferritin-positive microglia were rarely found in control animals, but they occurred frequently throughout the CNS of virus-infected rats (Figs. 6, 7). Ferritin-positive microglia were found scattered randomly throughout a given section and showed no predilection to any particular brain area. Focal upregulation of ferritin expression was observed in various locations throughout the virus-infected CNS including cerebellum, cortex, and midbrain (Fig. 6). Overall, ferritin-positive microglia comprised a relatively small subset of all microglial cells, as visualized by double labeling with OX-42 and ferritin (Fig. 6C). Most of the ferritin-positive microglia did not show the hypertrophic morphology that is characteristic of activated microglia, but instead were dystrophic, displaying abnormally shaped cytoplasmic processes (Figs. 6D-F). Interestingly, despite their non-activated morphology some but not all ferritin-positive microglia showed intracytoplasmic ED1 positivity indicative of phagocytotic activity, as revealed by double immunofluorescent labeling of ferritin and ED1 (Fig. 6F). Similarly, some but not all of the ED1-positive microglia expressed ferritin (not shown). A most interesting finding was the intense ferritin labeling localized selectively to both red nuclei in the midbrain in some of the PVC-infected animals after 14, 21, or 28 dpi (Fig. 7). In some extreme cases, all rubrospinal neurons had completely degenerated since none could be visualized using cresyl violet staining. Instead of neuronal cell bodies, cresyl violet staining revealed nuclei typical of polymorphonuclear phagocytes within an area of necrosis.

3. Discussion

3.1. Microglial reactivity serves as an indirect but sensitive marker for neuropathology

The neuronal pathology caused by neonatal infection of rats with PVC-211 MuLV and the underlying mechanisms have not been well defined. We believe that the motor problems in these animals are the result of malfunctioning lower and upper motor neurons. Although a loss of neurons and spongiform change were reported to accompany the disease (Li et al., 2009), there has been little direct evidence on the nature of pathological changes within neurons. Our own studies using Fluro Jade, and antibodies against ubiquitin, hyperphosphorylated tau or α-synuclein also failed to show neuronal pathology. Here we sought to identify sites of neuronal damage using microglial reactivity as an indirect marker. Consistent with prior studies (Hoffman et al., 1992; Wilt et al., 2000), our findings on microglial activation reveal that the brain areas most sensitive to the consequences of viral infection are the spinal cord and brainstem primarily. This preferential involvement of the hindbrain, including the selective loss of rubrospinal neurons, is consistent with the neurological symptoms present in infected animals. Furthermore, the onset of microglial activation correlated closely with the onset of symptoms, and thus we believe that microglial activation was triggered by neuronal disturbances, which is in line with the role of microglia as sensitive indicators of neuronal pathology (Kreutzberg, 1996). The fact that the presence of activated microglia was not closely correlated with presence of virus in microvessels clearly argues against a direct role of viral antigen in the induction of microgliosis and therefore indirectly supports the idea that it is primarily neuronal dysfunction that sets off microglial activation. Consistent with previously expressed views, our interpretation of the functional significance of the observed microgliosis is that it signifies a neuroprotective response attempting to contain and minimize neuronal damage (Streit et al., 1999; Streit, 2002).

3.2. Not all ED1-positive microglial cells are activated microglia

The use of multiple microglial markers in the current study has facilitated deeper insight into the functional roles that microglia play during brain pathology. While antibodies such as OX-42 and Iba1, directed against the CR3 complement receptor and the ionized calcium binding adaptor molecule 1, respectively, serve as excellent markers for visualizing all microglial cells regardless of the cells' activation state (Graeber et al., 1988; Graeber et al., 1998; Ito et al., 1998), constitutive expression of these microglial antigens does not allow one to easily ascribe functional meaning to enhanced expression of these antigens during development of a hypertrophic (activated) state. In contrast, expression of the lysosomal ED1 antigen in microglia carries a functional implication for altered cellular activity, namely, that an ED1-positive cell is engaged in phagocytosis. A number of prior studies by others have shown expression of the ED1 antigen on microglia-derived macrophages in various pathological scenarios, including retroviral CNS infections (Bauer et al., 1994; Graeber et al., 1990; Hansen et al., 2001; Mueller et al., 2007). However, it is important to point out that ED1 is not a universal marker for detecting activated microglia (Graeber et al., 1998), which is corroborated by our current findings showing expression of ED1 in some but not all activated (hypertrophic) microglia. Often in brain injury or disease microglia become activated but do not necessarily become phagocytic, and thus the ED1 antibody is useful for making the distinction between activated phagocytic ($Iba1^+/OX\text{-}42^+$ and $ED1^+$) and activated non-phagocytic ($Iba1^+/OX\text{-}42^+$ and $ED1^-$) cells. It is useful also for differentiating blood-derived, constitutive macrophages from activated microglial cells (Milligan et al., 1991b). In a developmental context ED1 is important for distinguishing ameboid (immature) microglia which express the ED1 antigen and are present until about postnatal day 21 (Domaradzka-Pytel et al., 2000; Milligan et al., 1991a). Ameboid microglia represent the progeny of fetal macrophages, embryonic microglial precursor cells that begin to colonize the brain during early development (Streit, 2001). During postnatal development ameboid microglia differentiate into mature, ramified microglia (Ling and Wong, 1993), and concomitant with this final differentiation ameboid cells lose their macrophage characteristics, which includes loss of the ED1 antigen. The developmentally regulated disappearance of ED1-positive ameboid cells coincides with the previously reported disappearance of ED1-positive cells in PVC-211-infected neonatal rats suggesting that in previous studies the identification of ED1-positive cells could have included ameboid as well as “activated microglia”(Wilt et al., 2000). However, we believe that the current study has served to clarify this issue.

3.3. Ferritin-positive microglial cells are mostly but not all dystrophic microglia

A second functional marker employed in our investigation to study the mechanism underlying viral infection is ferritin, the well-known iron storage protein. While ferritin is expressed in a number of CNS cells, including neurons and oligodendrocytes, its recently described prevalence in dystrophic microglia has focused attention on the possibility that iron-mediated oxidative stress could be a factor contributing to microglial deterioration in the context of neurodegenerative diseases (Lopes et al., 2008; Simmons et al., 2007). Specifically, we observed in human brain that morphologically abnormal microglial cells, termed dystrophic microglia (Streit et al., 2004), were frequently positive for ferritin (Lopes et al., 2008), leading us to propose that iron-mediated oxidative stress may be a factor contributing to the structural deterioration (dystrophy) of microglial cells. Microglia are the most readily available source of brain macrophages and involved in the elimination and clean-up of tissue debris after injury, and they may be involved in the sequestration and elimination of excess iron that enters into the CNS, which causes the cells to express ferritin. We observed an upregulation of ferritin expression after viral infection compared with control animals, and that ferritin expression occurred seemingly at random throughout the CNS. For the most part, ferritin expression on microglia was not very intense in that non-activated cells were labeled and that even in those regions showing conspicuous microglial activation ferritin-positive cells made up only a small

proportion of the total microglia. We found ferritin expressed in some activated phagocytic microglia, as evidenced by coexpression of both ferritin and ED1 antigen (Fig. 6F), as well as in some dystrophic cells (Fig. 6E). Our interpretation of these findings is that ferritin upregulation is a mechanism by which microglia divert iron-mediated free radical damage away from neurons and other nonrenewable cells in the CNS, but as iron accumulates intracellularly microglia themselves are exposed to iron-mediated damage and as a result develop a dystrophic morphology. A very intriguing observation was the full-blown necrotic degeneration of both red nuclei accompanied by a dense accumulation of ferritin-positive, and seemingly dystrophic microglia. Since the red nucleus is a constitutively iron-rich region in the developing rat brain (Roskams and Connor, 1994), we suspect that viral infection of endothelial cells in this region caused endothelial cell injury and/or lysis resulting in hemorrhagic necrosis which triggered a massive microglial response. The influx of erythrocytes together with high endogenous iron in the red nucleus produced a local iron overload and excessive iron-mediated oxidative stress that killed rubrospinal neurons. The disruption of endothelial cell membranes and tight junctions has been reported in the CNS of rats infected with PVC-441 (Saida et al., 1997), a viral clone isolated alongside PVC-211 (Kai and Furuta, 1984).

In summary, the current study represents an in-depth histopathological analysis of reactive microgliosis in the PVC-211-induced neurodegenerative syndrome. The results underscore the importance of detecting activated microglia as a measure of CNS dysfunction and the multifaceted roles theses cells serve in the preservation of CNS homeostasis.

4. Experimental procedures

All procedures were performed according to protocols approved by the University of Florida Institutional Use and Care of Animals Committee (IUCAC).

4.1. Animals and tissue processing

Pregnant F344 rats were obtained from Charles River (Raleigh, NC) and housed under standard SPF conditions in the McKnight Brain Institute animal care facility. Newborn rat pups no older than 2 days received intracranial inoculation of PVC-211 MuLV in DMEM (Gibco, 11995), as described previously (Wilt et al., 2000). Control animals were injected with virus–free culture media. The infected pups were returned to the dam and observed for neurologic disease symptoms such as spastic paraparesis, ataxia, loss of splay reflex, tremor, and paralysis (Hoffman et al., 1992; Wilt et al., 2000). Animals were sacrificed at 7, 14, 21, and 28dpi. A total of thirty-eight rats were used in the current study, six animals in each experimental group and four animals in each control group, except for the 7dpi control group which consisted of two animals. Of the six animals in each experimental group four were used for preparing cryostat sections and two for vibratome sections. Of the four animals in each control group three were used for cryostat sections and one for vibratome sections. Both animals in the 7dpi control group were used for cryostat sections only.

Animals were deeply anesthetized with sodium pentobarbital (Beuthanasia-D, Schering-Plough Animal Health) and perfused transcardially with 0.1 M phosphate-buffered saline (PBS; pH 7.4) followed by a fixative solution containing 4% paraformaldehyde in PBS. The brains and spinal cords were removed and fixed by immersion in the same fixative for an additional 2-4 hours for cryostat sections, or post-fixed 7 months for vibratome sections. Tissues were washed with PBS after fixation. Prior to cryosectioning, tissues were cryoprotected using 30% sucrose in PBS for 2 days. Frozen sections of the brain and spinal cord were cut on a cryostat at 20μm thickness. For vibratome sectioning, tissues were embedded with 3% agarose in water and cut at 50μm thickness.

4.2. Immunohistochemical procedures

Two primary antibodies were used for labeling all microglial cells: mouse anti-rat CD11b antibody, OX-42, and Iba1, directed against the ionized calcium binding adaptor molecule 1 (Table 1). Other antibodies used for characterizing activated microglia and studying the relationship between microglia and other components included NeuN, Ferritin, gp70, ED1, α-synuclein, and PHF tau (Table 1). OX-42 and ferritin were the only two antibodies that were visualized using both horseradish peroxidase-based immunohistochemistry and immunofluorescent staining. All other primary antibodies were visualized using immunofluorescence only.

For immunostaining using peroxidase-based procedures, sections were incubated in blocking buffer containing 10% goat serum, 0.1% Triton X-100 in PBS for 1 hr at 37 °C before applying the primary antibodies. Primary antibodies, diluted in PBS containing 5% goat serum and 0.1% Triton X-100 in PBS, were applied to sections in a moist chamber and incubated overnight at 4°C. After several washes, sections were incubated with either a biotinylated goat anti-mouse IgG (Vector Laboratories, Inc., BA-9200) or a biotinylated goat anti-rabbit IgG secondary antibody (Vector, BA-1000), diluted at 1:500, for 1 hr at room temperature. Sections were then incubated with Avidin D conjugated to horseradish peroxidase (Vector, A-2004), and visualized using DAB-H_2O_2 substrate (Fast 3,3′-diaminobenzidine tablet sets, Sigma D-4293). Some sections were counterstained with 0.5% cresyl violet after immunostaining. All slides were dehydrated through ascending alcohols, cleared in xylenes and coverslipped with Permount.

For fluorescent immunolabeling, sections were blocked with blocking buffer and incubated with the primary antibody followed by several washes and incubation with appropriate secondary fluorescent antibodies. For double labeling of different antigens in the same section, a combination of primary antibodies was applied to sections as cocktail primary antibodies. Cocktail secondary antibodies were then used for visualizing binding sites of primary antibodies. All monoclonal primary antibodies were visualized using goat anti-mouse IgG conjugated with either Alexa Fluor 488 (Molecular probes, A11029; Eugene, OR; used at a dilution of 1:400 or 1:500) or Alexa Fluor 568 (Molecular probes, A11004; diluted at 1:300), as well as donkey anti-mouse IgG conjugated with Alexa Fluor 488 (Molecular probes, A21202; diluted at 1:300). Polyclonal primary antibodies were visualized using goat anti-rabbit IgG conjugated with either Alexa Fluor 594 (Molecular probes, A11012; diluted at 1:400) or Alexa Fluor 488 (Molecular probes, A11034, diluted at 1:400; A11008, diluted at 1:300), as well as donkey anti-rabbit IgG conjugated with Alexa Fluor 488 (Molecular probes, A21206, diluted at 1:300). Viral gp70 was visualized using donkey anti-goat IgG conjugated with Alexa Fluor 594 (Molecular probes, A11058, diluted at 1:400). Sections were coverslipped with GEL/MOUNT (Biomeda Corp.; Foster City, CA, M01).

4.3. Lectin histochemistry

Besides using immunohistochemical labeling of microglial cells on cryostat sections, lectin histochemistry was also used to label microglia on vibratome sections. Prior to staining, sections were treated with 0.9% H_2O_2 in PBS for 30min at room temperature for quenching the endogenous peroxidase, 0.5%Triton in PBS for 30min at room temperature, and then Pepsin for 30min at 37°C. Sections were incubated with isolectin B4 (peroxidase labeled, Sigma, L-5391, diluted at 1:200 in 0.1% Triton/PBS) for overnight at 4°C. After washing, the binding was visualized by $CoCl_2$-DAB-H_2O_2 in 0.1% Triton/PBS. Sections were mounted onto glass slides, extra solutions drained, dehydrated and cleared before being coverslipped with Permount.

4.4. Fluoro-Jade histochemistry

In order to identify degenerating neurons, Fluoro-Jade B histochemical staining was performed. Cryostat sections were thawed and air-dried for 30min at 37°C, followed by immersion in 100% and 70% ethanol for 3 min each. The sections were then immersed in a solution containing 1% sodium hydroxide in 80% ethanol for 5 min, and rinsed in 70% ethanol and deionized water for 3 min each. After an incubation in 0.06% $KMnO_4$ solution for 20 min, followed by a rinse in deionized water for 3 min, the sections were stained with 0.0004% Fluoro-Jade B (Chemicon, Temecula, CA, AG310) in 0.1% acetic acid solution for 30 min. The sections were rinsed in deionized water three times, 5min each, air-dried, cleared in xylene, and then coverslipped with Permount.

4.5. Observation and imaging

Slides were examined with a Zeiss Axioskop 2 microscope. Digital images were captured with a Spot Slider 3 digital camera (Diagnostic Instruments Inc.; Sterling Heights, MI). In double-immunofluorescent preparations, micrographs were prepared using images pseudo-colored or digitally merged from images captured at single fluorochrome using Adobe Photoshop software (Adobe Systems Inc.; San Jose, CA).

Acknowledgments

This work was supported in part by NIH grant AG023665 and by a merit review award from the Office of Research and Development, Department of Veterans Affairs.

References

Bauer J, Sminia T, Wouterlood FG, Dijkstra CD. Phagocytic activity of macrophages and microglial cells during the course of acute and chronic relapsing experimental autoimmune encephalomyelitis. J Neurosci Res 1994;38:365–75. [PubMed: 7932870]

Dijkstra CD, Dopp EA, Joling P, Kraal G. The heterogeneity of mononuclear phagocytes in lymphoid organs: distinct macrophage subpopulations in the rat recognized by monoclonal antibodies ED1, ED2 and ED3. Immunology 1985;54:589–99. [PubMed: 3882559]

Domaradzka-Pytel B, Ludkiewicz B, Jagalska-Majewska H, Morys J. Immunohistochemical study of microglial and astroglial cells during postnatal development of rat striatum. Folia Morphol (Warsz) 2000;58:315–23. [PubMed: 11000888]

Gorter JA, Mesquita AR, van Vliet EA, da Silva FH, Aronica E. Increased expression of ferritin, an iron-storage protein, in specific regions of the parahippocampal cortex of epileptic rats. Epilepsia 2005;46:1371–9. [PubMed: 16146431]

Graeber MB, Streit WJ, Kreutzberg GW. Axotomy of the rat facial nerve leads to increased CR3 complement receptor expression by activated microglial cells. J Neurosci Res 1988;21:18–24. [PubMed: 3216409]

Graeber MB, Streit WJ, Kiefer R, Schoen SW, Kreutzberg GW. New expression of myelomonocytic antigens by microglia and perivascular cells following lethal motor neuron injury. J Neuroimmunol 1990;27:121–32. [PubMed: 2332482]

Graeber MB, Lopez-Redondo F, Ikoma E, Ishikawa M, Imai Y, Nakajima K, Kreutzberg GW, Kohsaka S. The microglia/macrophage response in the neonatal rat facial nucleus following axotomy. Brain Res 1998;813:241–53. [PubMed: 9838143]

Hansen R, Sauder C, Czub S, Bachmann E, Schimmer S, Hegyi A, Czub M. Activation of microglia cells is dispensable for the induction of rat retroviral spongiform encephalopathy. J Neurovirol 2001;7:501–10. [PubMed: 11704882]

Hoffman PM, Cimino EF, Robbins DS, Broadwell RD, Powers JM, Ruscetti SK. Cellular tropism and localization in the rodent nervous system of a neuropathogenic variant of Friend murine leukemia virus. Lab Invest 1992;67:314–21. [PubMed: 1405490]

Ishimaru H, Ishikawa K, Ohe Y, Takahashi A, Tatemoto K, Maruyama Y. Activation of iron handling system within the gerbil hippocampus after cerebral ischemia. Brain Res 1996;726:23–30. [PubMed: 8836541]

Ito D, Imai Y, Ohsawa K, Nakajima K, Fukuuchi Y, Kohsaka S. Microglia-specific localisation of a novel calcium binding protein, Iba1. Brain Res Mol Brain Res 1998;57:1–9. [PubMed: 9630473]

Kai K, Furuta T. Isolation of paralysis-inducing murine leukemia viruses from Friend virus passaged in rats. J Virol 1984;50:970–3. [PubMed: 6328027]

Kaur C, Singh J, Ling EA. Immunohistochemical and lectin-labelling studies of the distribution and development of microglia in the spinal cord of postnatal rats. Arch Histol Cytol 1993;56:475–84. [PubMed: 8129981]

Kreutzberg GW. Microglia: a sensor for pathological events in the CNS. Trends Neurosci 1996;19:312–8. [PubMed: 8843599]

Li X, Hanson C, Cmarik JL, Ruscetti S. Neurodegeneration induced by PVC-211 murine leukemia virus is associated with increased levels of vascular endothelial growth factor and macrophage inflammatory protein 1 alpha and is inhibited by blocking activation of microglia. J Virol 2009;83:4912–22. [PubMed: 19279110]

Ling EA, Wong WC. The origin and nature of ramified and amoeboid microglia: a historical review and current concepts. Glia 1993;7:9–18. [PubMed: 8423067]

Lopes KO, Sparks DL, Streit WJ. Microglial dystrophy in the aged and Alzheimer's disease brain is associated with ferritin immunoreactivity. Glia 2008;56:1048–60. [PubMed: 18442088]

Milligan CE, Cunningham TJ, Levitt P. Differential immunochemical markers reveal the normal distribution of brain macrophages and microglia in the developing rat brain. J Comp Neurol 1991a; 314:125–35. [PubMed: 1797868]

Milligan CE, Levitt P, Cunningham TJ. Brain macrophages and microglia respond differently to lesions of the developing and adult visual system. J Comp Neurol 1991b;314:136–46. [PubMed: 1797869]

Mueller CA, Schluesener HJ, Fauser U, Conrad S, Schwab JM. Lesional expression of the endogenous angiogenesis inhibitor endostatin/collagen XVIII following traumatic brain injury (TBI). Exp Neurol 2007;208:228–37. [PubMed: 17942095]

Roskams AJ, Connor JR. Iron, transferrin, and ferritin in the rat brain during development and aging. J Neurochem 1994;63:709–16. [PubMed: 8035195]

Saida K, Saida T, Kai K, Iwamura K. Central nervous system lesions in rats infected with Friend murine leukemia virus-related PVC441: ultrastructural and immunohistochemical studies. Acta Neuropathol 1997;93:369–78. [PubMed: 9113202]

Simmons DA, Casale M, Alcon B, Pham N, Narayan N, Lynch G. Ferritin accumulation in dystrophic microglia is an early event in the development of Huntington's disease. Glia 2007;55:1074–1084. [PubMed: 17551926]

Streit WJ, Walter SA, Pennell NA. Reactive microgliosis. Prog Neurobiol 1999;57:563–81. [PubMed: 10221782]

Streit WJ. Microglia and macrophages in the developing. CNS Neurotoxicology 2001;22:619–24.

Streit WJ. Microglia as neuroprotective, immunocompetent cells of the CNS. Glia 2002;40:133–9. [PubMed: 12379901]

Streit WJ, Sammons NW, Kuhns AJ, Sparks DL. Dystrophic microglia in the aging human brain. Glia 2004;45:208–12. [PubMed: 14730714]

Streit WJ, Braak H, Xue QS, Bechmann I. Dystrophic (senescent) rather than activated microglial cells are associated with tau pathology and likely precede neurodegeneration in Alzheimer's disease. Acta Neuropathol 2009;118:475–85. [PubMed: 19513731]

Wilt SG, Dugger NV, Hitt ND, Hoffman PM. Evidence for oxidative damage in a murine leukemia virus-induced neurodegeneration. J Neurosci Res 2000;62:440–50. [PubMed: 11054813]

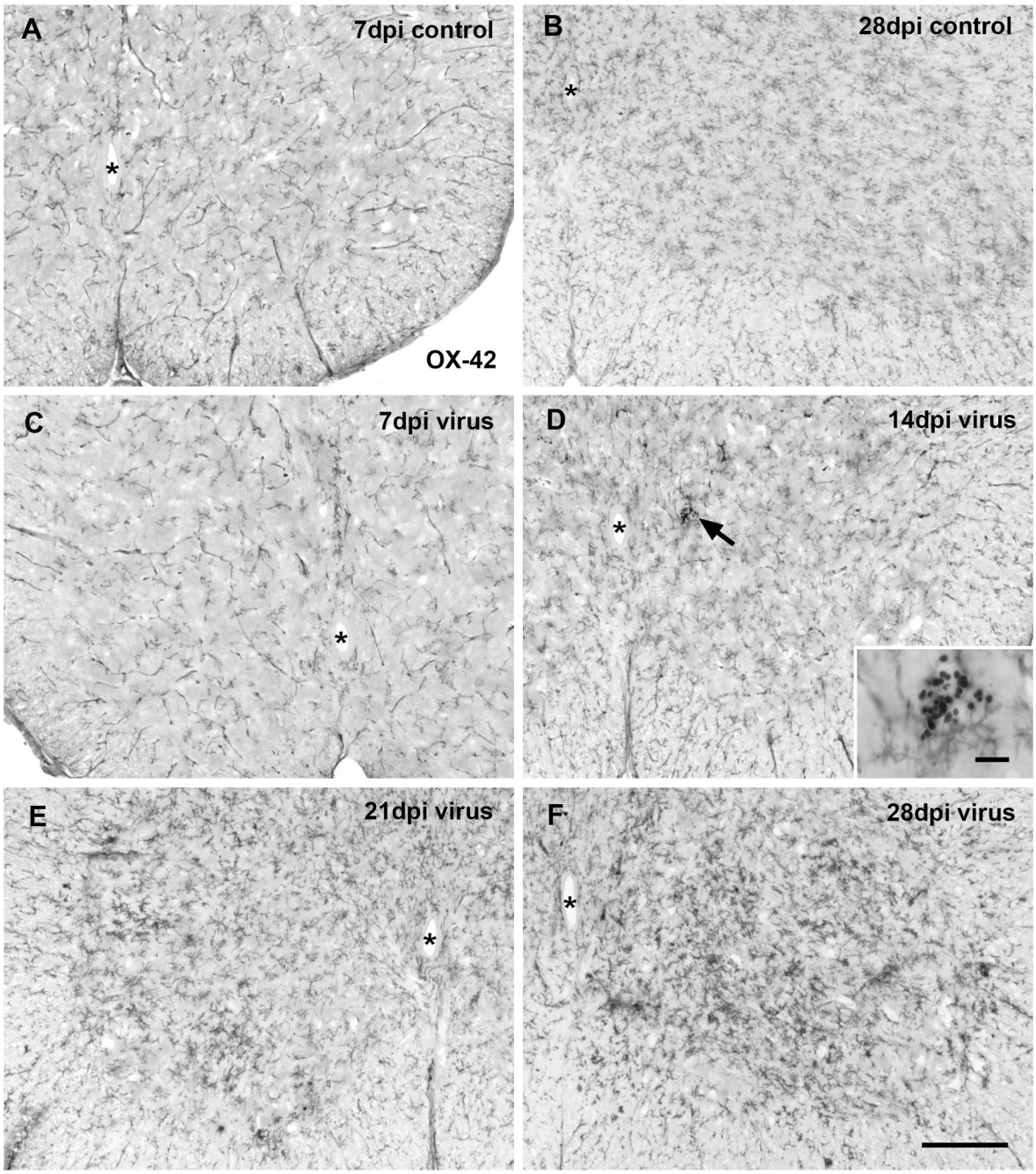

Fig. 1.

Microglia immunolabeled with OX-42 in the rat spinal cord ventral horn at different times after intracranial PVC-211 injection. (A, B) Sections from controls show normal distribution of microglia at 7 and 28 dpi. Note the increases in cell number and in differentiation during this period of postnatal development. (C-F) Virus infection does not result in apparent microglial activation at 7 and 14 dpi. A small intraparenchymal hemorrhage revealing peroxidase-positive erythrocytes is encountered in the spinal gray matter at 14 dpi without activated microglia nearby (arrow in D; enlarged in inset). Microglial activation is conspicuous in the spinal cord gray matter at 21 dpi (E) and has intensified by 28 dpi (F). Animals showed paresis (E) and

paralysis (F) of hind limbs. Asterisks indicate central canal. Scale bar in F for all, 200 μm; inset, 20 μm.

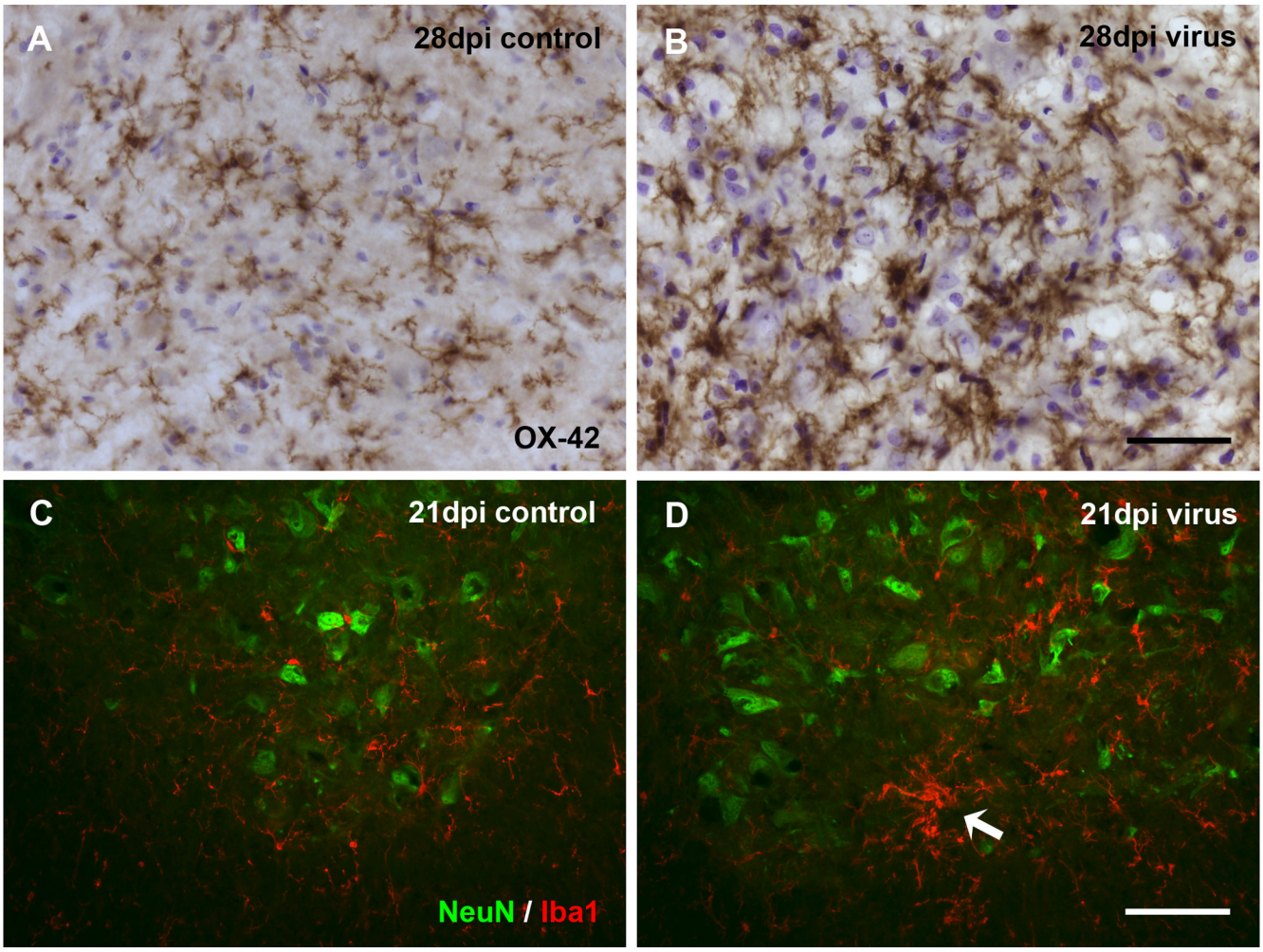

Fig. 2.

Detail of microglial activation in spinal cord ventral horn and relationship to neurons. (A, B) Comparison of control and virus–infected tissue reveals more intense staining of hypertrophic microglia with OX-42. Cresyl violet counterstain. (C, D) Double immunofluorescent staining for neurons (NeuN, green) and microglia (Iba1, red) in control (C) and virus-infected (D) animals. Activated microglia are intermingled with normal appearing neurons in D. Arrow points to cluster of activated cells. Animals showed paresis (D) and paralysis (B) of hind limbs. Scale bar, 50 μm in B for A and B; 100 μm in D for C and D.

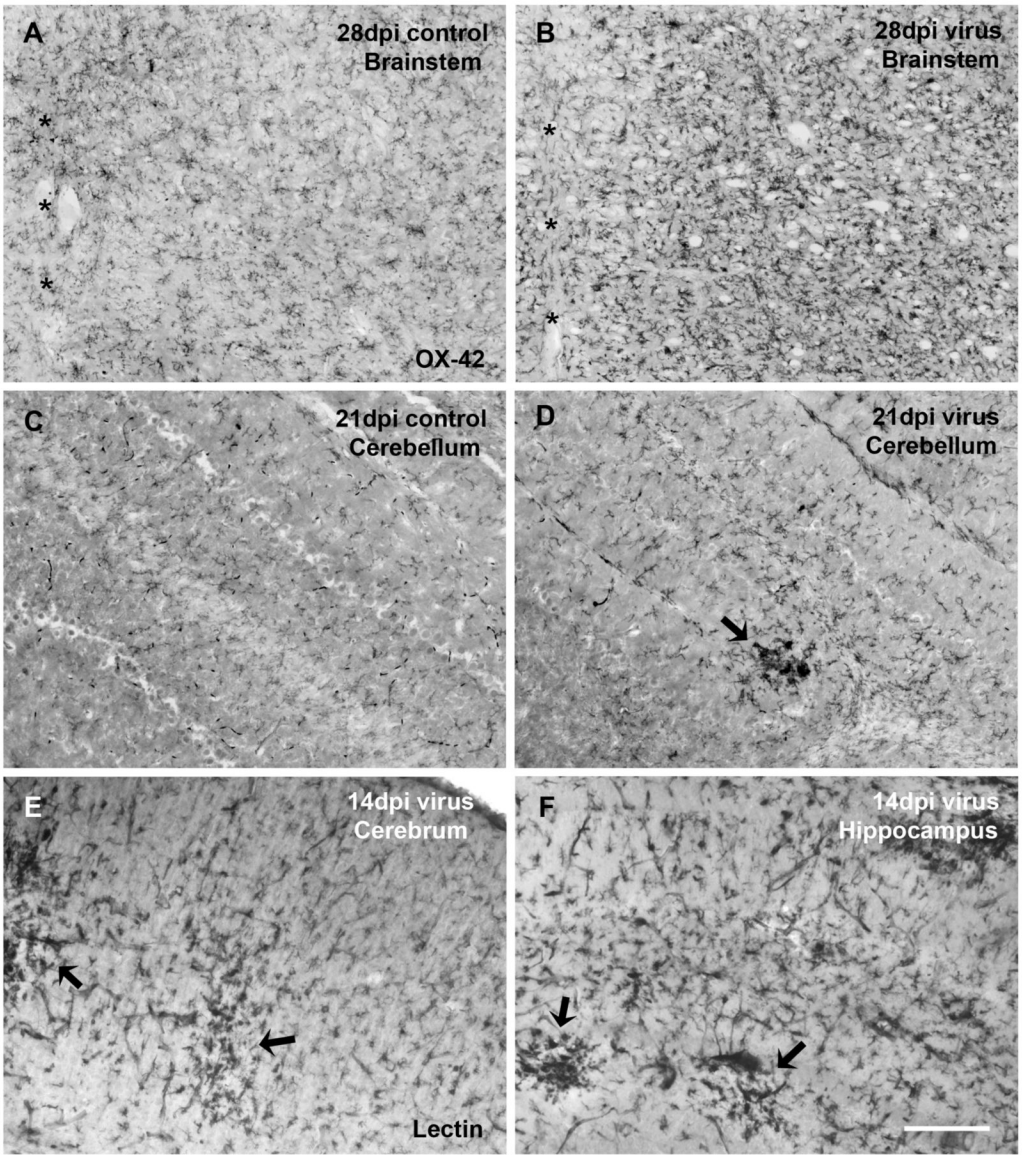

Fig. 3.

Besides the spinal cord, brainstem is another virus infection-sensitive brain area displaying evident microglial activation (A, B), asterisks indicating the midline. Microglial activation is generally less pronounced in the cerebral cortex, cerebellum, and other brain areas. However, clusters of activated microglia can be occasionally encountered in these areas, as exampled in virus-infected cerebellum (D), cerebral cortex (E), and hippocampus (F). (C) Cerebellum of a control animal at 21 dpi shows no microglial activation. (A-D) Microglia are immunolabeled with OX-42. (E, F) Microglia are labeled by lectin histochemistry. Scale bar, 200 μm.

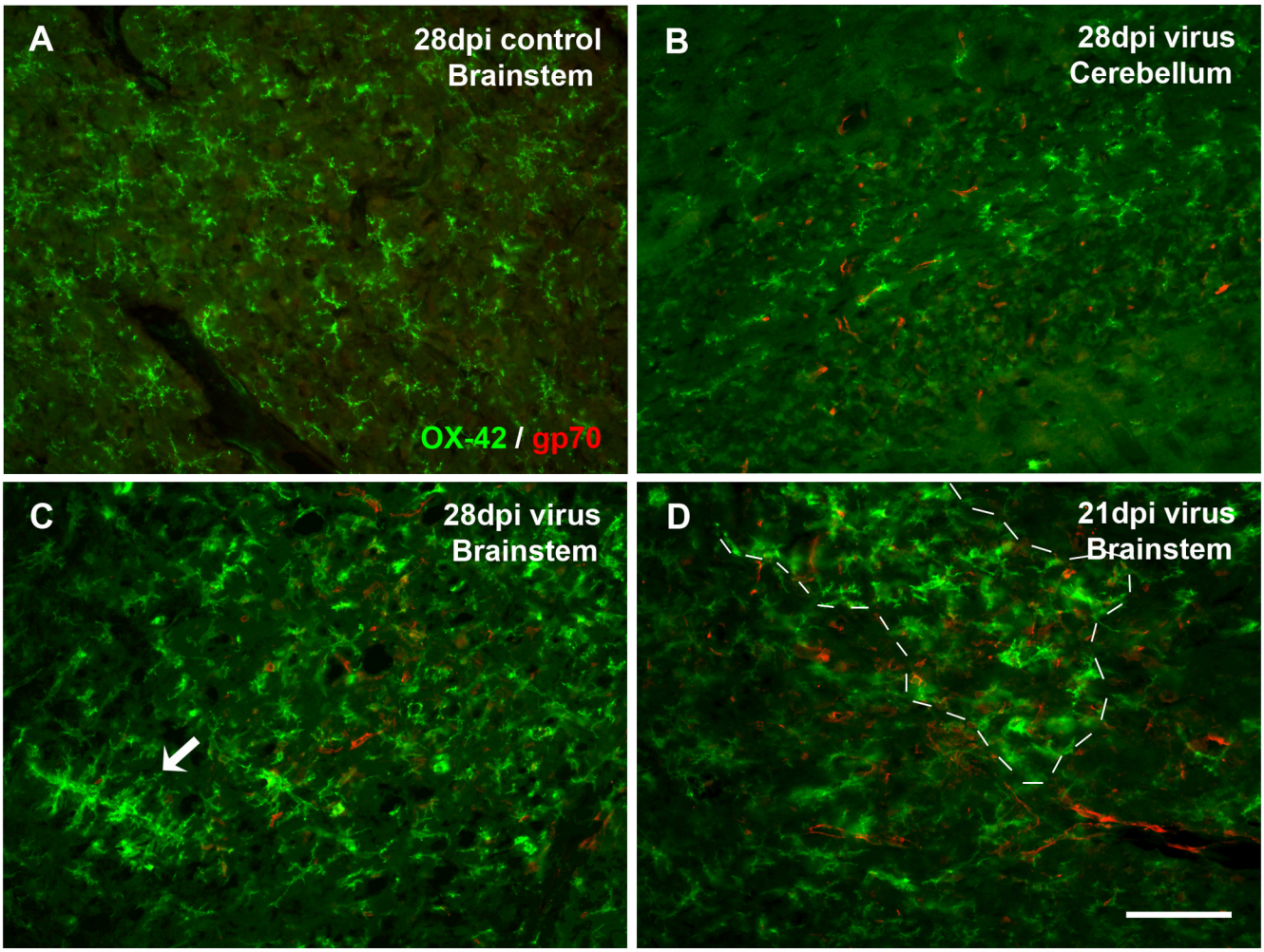

Fig. 4.

Double immunofluorescent staining for microglia (OX-42) and viral gp70 reveals lack of direct correlation between presence of activated microglia and PVC-211-infected endothelial cells. (A) Absence of gp70 immunoreactivity in the brainstem of a control rat. (B) A virus-infected cerebellum with virus infection but no microglial activation. (C, D) Virus-infected brainstems, with universal gp70 labeling while activated microglia in confined areas. (C) Activated microglia are spread diffusely throughout the field, with some aggregates (arrow), but do not accumulate around gp70-positive blood vessels. (D) Both resting and activated microglia (area of activation delineated by dashed line) are colocalized with widespread gp70 immunoreactivity in microvessels. Scale bar, 100 μm.

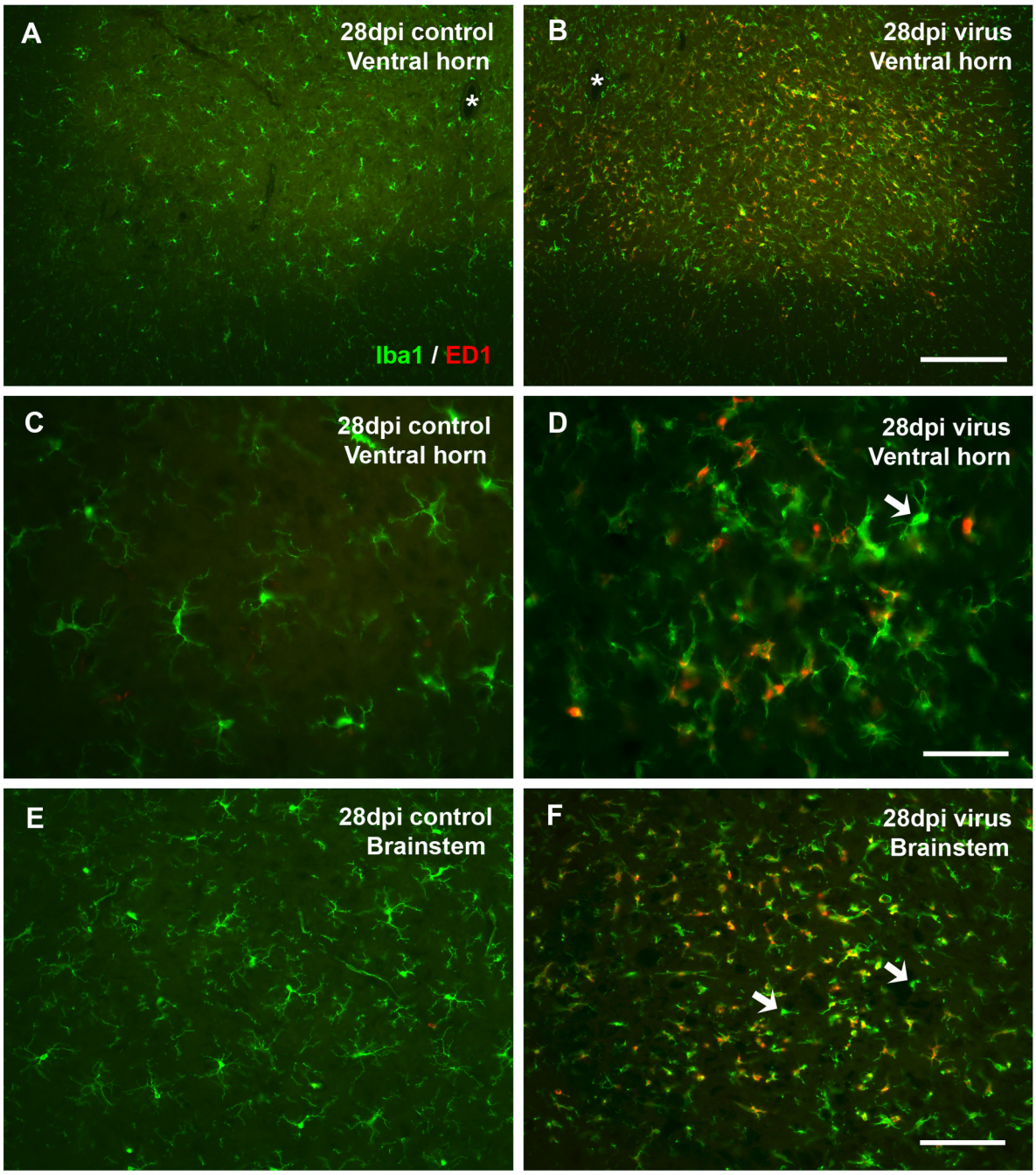

Fig. 5.

Characterization of microglia by double immunolabeling with Iba1 and ED1 in spinal cord ventral horn (A-D) and brainstem (E, F) shows increased ED1 immunoreactivity present in some but not all activated microglia. Control tissue shows a lack of ED1 staining in non-activated ramified microglia stained with Iba1 (A, C, E). ED1 staining is prominent in virus-infected spinal cord and brainstem, merged images (B, D, F) and colocalized mostly with activated microglia (D). However, not all activated microglia are ED1-positive. Arrows in D and F indicate activated microglia lacking ED1 staining. Asterisks indicate central canal. Scale bar, 200 μm in B for A and B, 50 μm in D for C and D, 100 μm in F for E and F.

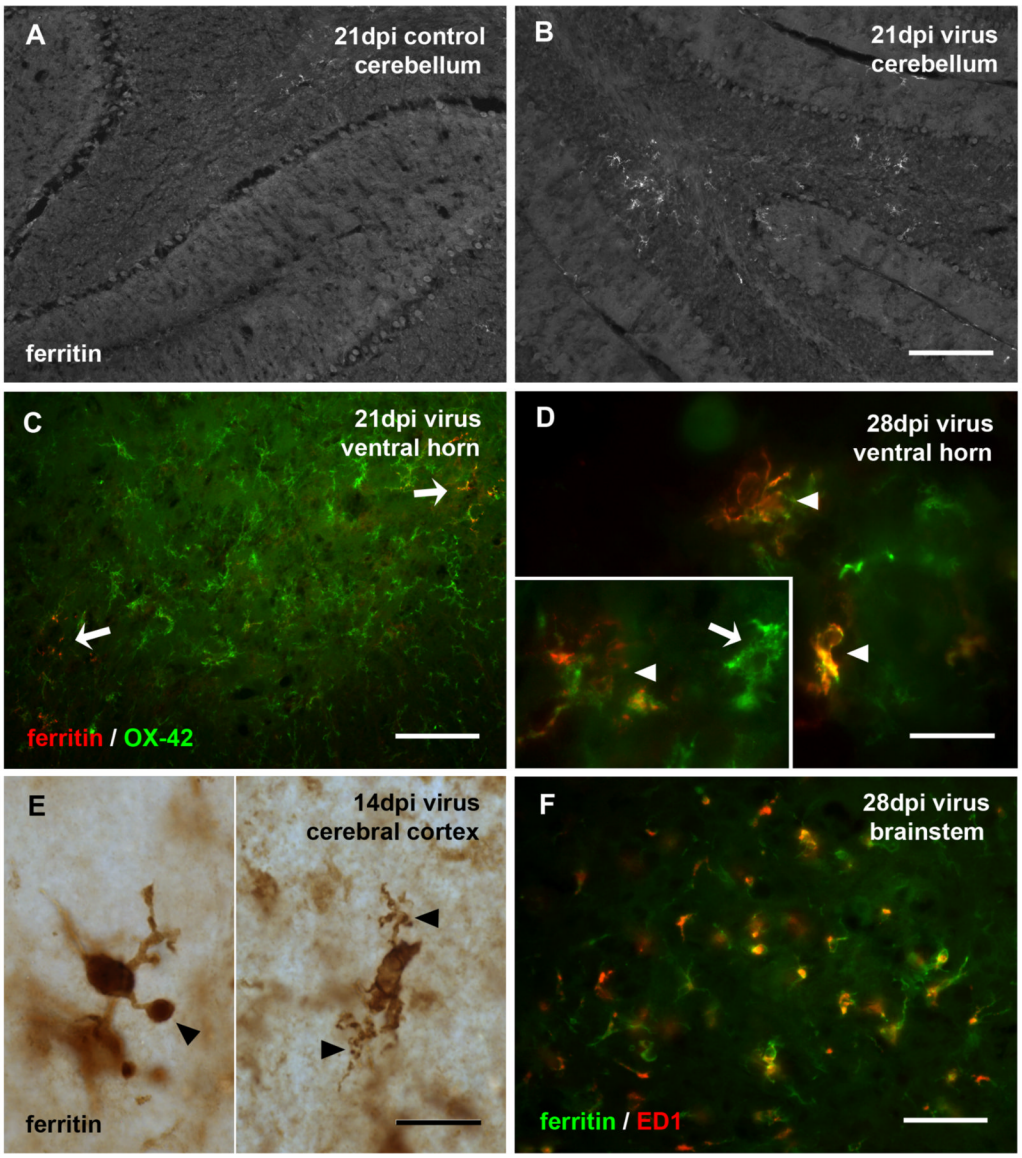

Fig. 6.

Expression of ferritin is increased following viral infection and associated with dystrophic microglia. (A, B) Low power view of the cerebellum in control and infected rats shows increased ferritin staining of microglia in the cerebellum. Ferritin-positive microglia in virus-infected spinal cord shows them to be a small subset of OX-42-positive cells (C, pointed by arrows). Double-labeling with anti-ferritin and OX-42 in spinal cord ventral horn (D) or single immunolabeling by ferritin in cerebral cortex (E, pieced together from two views) reveals them to exhibit microglial dystrophy evident as short, tortuous and fragmented cytoplasmic processes (arrowheads in D-E, and inset in D). The inset in D shows a hypertrophic OX-42-positive cell that is negative for ferritin (arrow). Double-labeling with anti-ferritin and ED1 in the brainstem (F) shows ED1 immunoreactivity present in some ferritin-positive microglia. Scale bar, 200 μm in B for A and B, 100 μm in C, 20 μm in D-E and inset, 50 μm in F.

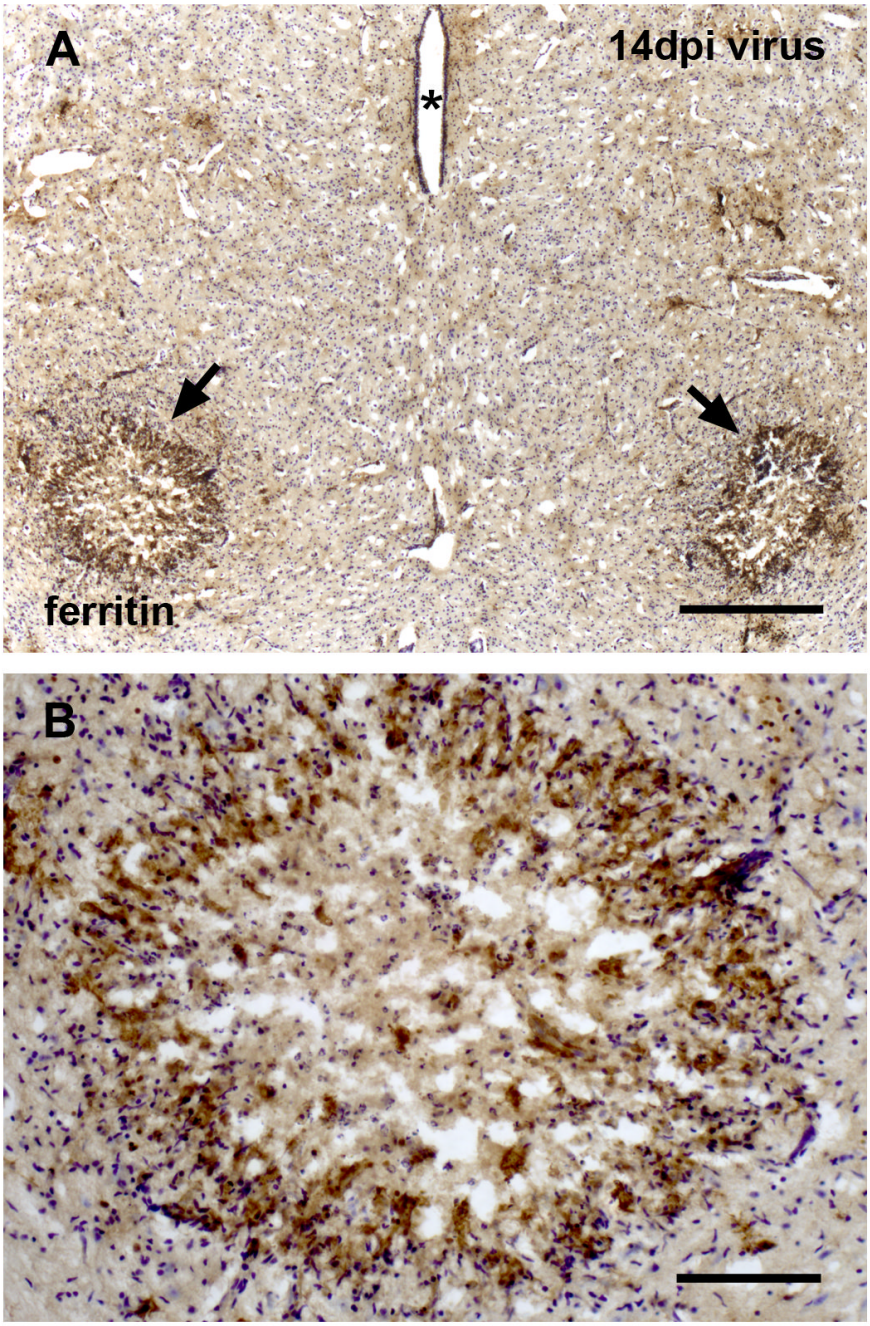

Fig. 7.

Selective degeneration of the red nuclei in midbrain is associated with intense ferritin immunoreactivity. (A) Localized increases in ferritin staining are evident in red nucleus areas bilaterally (arrows), aterisks indicating the cerebral aqueduct. (B) High magnification reveals necrosis and loss of rubrospinal neurons. The intensely immunoreactive perimeter is characterized by hypercellularity, and immunorecative cells likely represent degenerating microglia, cresyl violet counterstain. Scale bar, 400 μm in A, 100 μm in B.

Table 1

Primary antibodies used in immunohistochemical studies

Primary antibodies	Isotypes; Dilution	Suppliers
OX-42 (mouse anti-rat CD11b)	MAb; I g G; 1:400	SeroTec, MCA275G
Iba1 (rabbit anti-Iba1)	PAb; IgG; 1:500	Wako, 019-19741
NeuN (mouse anti-neuronal nuclei)	MAb; IgG; 1:200	Chemicon, MAB377
Ferritin (rabbit anti-human spleen ferritin)	PAb; IgG; 1:1000	Sigma, F5012
Ferritin (rabbit anti-horse spleen ferritin)	PAb; IgG; 1:800	Sigma, F6136
gp70 (goat anti-viral gp70)	IgG; 1:200	NCI Repository
ED1 (mouse anti-rat monocytes/macrophages [CD68])	MAb; IgG; 1:300	Chemicon; MAB1435